Chinese Chemical Letters 34 (2023) 107495

Contents lists available at ScienceDirect

Chinese Chemical Letters

journal homepage: www.elsevier.com/locate/cclet

Enhancing the performance of organic solar cells by modification of cathode with a self-assembled monolayer of aromatic organophosphonic acid

Wenlong Liu[a], Hao Lu[b], Yan Zhang[b], Hao Huang[b], Xinming Zheng[b], Yahui Liu[c], Youzhi Wu[a,*], Xinjun Xu[b,*]

[a] School of Materials Science and Engineering, Lanzhou University of Technology, Lanzhou 730050, China
[b] Key Laboratory of Energy Conversion and Storage Materials, College of Chemistry, Beijing Normal University, Beijing 100875, China
[c] College of Textiles & Clothing, State Key Laboratory of Bio-fibers and Eco-textiles, Qingdao University, Qingdao 266071, China

ARTICLE INFO

Article history:
Received 31 March 2022
Revised 20 April 2022
Accepted 7 May 2022
Available online 11 May 2022

Keywords:
Organic solar cells
Interface modification
Self-assembled monolayer
Stability
PCE

ABSTRACT

We use a single-molecule self-assembled layer of an aromatic organophosphonic acid (2PACz) to modify the cathode interface layer in inverted organic solar cells (OSCs). The modified OSCs not only have an obvious improvement in power conversion efficiency (PCE), but also demonstrate greatly enhanced air stability. Ultraviolet photoelectron spectroscopy shows that the work function of cathode interlayer after modification by 2PACz is more suitable for electron extraction. In addition, the surface energy is reduced without affecting the film deposition, which will be beneficial to reduce the interfacial traps. As a result, the PCE of OSCs based on the PBDB-T:IT-M system is increased, and its stability in air is greatly improved (remaining 88% of its initial PCE after 555 h in air). Therefore, we provide a new strategy for constructing high-performance non-fullerene OSCs with enhanced air stability.

Organic solar cells (OSCs) have attracted a considerable attention in the last decade on account of their potentials such as flexibility, light-weight and capability of being manufactured over large areas [1–3]. With the development of organic photovoltaic materials, especially non-fullerene acceptors, the power conversion efficiency (PCE) of OSCs has been improved rapidly [4–6]. OSCs can be divided into two typical device architectures, namely conventional and inverted ones, according to their polarity. In the conventional structure, the holes move toward the bottom electrode and the electrons move toward the top electrode, which become reverse in the inverted one. Currently, most high-efficiency non-fullerene OSCs utilize a conventional device structure which employs poly(3,4-ethylenedioxythiophene):polystyrene sulfonate (PEDOT:PSS) as a hole extraction layer on the bottom electrode together with an ultrathin water-/alcohol-soluble interlayer between the active layer and the top electrode to facilitate electron extraction. The water-soluble/alcohol-soluble active layer is sandwiched between the top electrode to facilitate electron extraction, and achieves outstanding device efficiency in conventional devices [7]. Although PEDOT:PSS has a high work function of 5.2 eV and a good hole transport ability to help the extraction of holes, its strong acidity and hygroscopicity associate with deterioration of device stability [8]. The situation is similar for the ultrathin water/alcohol soluble interlayer adjacent to the top electrode, which also suffers from hygroscopicity [9]. In contrast, the inverted device architecture shows a better stability because of using stable metal oxides as charge extraction layers [10]. In inverted OSCs, typically ZnO is served as the electron extraction layer (EEL) on the bottom electrode owing to its advantages of high electron mobility, excellent optical transparency and adjustable electro-optic properties [11]. Due to the inherent energy barrier between each layer in OSCs, charge carriers will lose energy when they are transferred across the interfaces, thus affecting their transport process, especially for the collection of electrons [12]. In addition, lots of trap states usually exist at the interface after depositing the active layer onto the surface of ZnO EEL [13]. Therefore, optimizing the interface between the active layer and the EEL is an effective method to promote electron extraction and improve device efficiency and stability [14].

To this end, lots of attempts have been made by introducing an interface layer between the active layer and the ZnO layer [15]. Such an interface layer can be made of self-assembled dipolar small-molecule monolayers [16], fullerene derivatives [17], water/alcohol soluble non-conjugated polymers with amino groups

* Corresponding authors.
E-mail addresses: youzhiwu@163.com (Y. Wu), xuxj@bnu.edu.cn (X. Xu).

https://doi.org/10.1016/j.cclet.2022.05.009
1001-8417/

[18], polymer nanodots [19] and conjugated polyelectrolytes [20]. It should be noted that despite these interfacial modification layers can improve the performance of fullerene OSCs, they may not be directly transferred to non-fullerene ones. For instance, poly[(9,9-bis(3′-(*N*,*N*-dimethylamino)propyl)−2,7-fluorene)-*alt*-2,7-(9,9-dioctylfluorene)] (PFN) is a widely used interface layer to effectively improve electron extraction in fullerene OSCs, the electron extraction worsens in non-fullerene systems, resulting in S-shaped current-voltage curves [21]. Another example is polyethyleneimine ethoxylated (PEIE), it may cause a chemical reaction with certain non-fullerene acceptors such as 3,9-bis(2-methylene-(3-(1,1-dicyanomethylene)-indanone))−5,5,11,11-tetrakis(4-hexylphenyl)-dithieno[2,3-*d*:2′,3′-*d*']-*s*-indaceno[1,2-*b*:5,6-*b*']dithiophene (ITIC) to disrupt the electronic structure of acceptor molecules, and thus interferes with intramolecular charge transfer and restricts its widely use in non-fullerene systems [22]. As a result, new interface layers compatible with non-fullerene systems and suitable for fabricating high-efficiency and stable OSCs are urgently desired.

In this work, we overcome this obstacle by using a self-assembled monolayer of aromatic organophosphonic acid (2PACz) as the interlayer. 2PACz is firstly reported by Steve Albrecht *et al*. in the field of perovskite cells, where it was used as a self-assembled monolayer (SAM) to replace the traditional hole transport layer 2,2′,7,7′-tetrakis[*N*,*N*-di(4-methoxyphenyl)amino]−9,9′-spirobifluorene (Spiro-OMeTAD) [23–25]. Recently, Lin *et al*. find it can also be applied in OSCs for anode modification to replace the hole transport material PEDOT:PSS [26]. We notice that phosphonic acid molecules can be anchored at the ITO surface through covalent binding in either monodentate, bidentate, or tridentate modes with the surface hydroxyl groups [27]. Similarly, ZnO modified by PEIE also has hydroxyl groups on its surface. So, we suppose that 2PACz will also cover the surface of PEIE to form a self-assembled monolayer through hydrogen bonding with hydroxyl groups of PEIE and leave the carbazole group towards active layer in OSCs to passivate the interface. Here, OSCs based on poly[(2,6-(4,8-bis(5-(2-ethylhexyl)thiophen-2-yl)-benzo[1,2-*b*:4,5-*b*']dithiophene))-*alt*-(5,5-(1′,3′-di-2-thienyl-5′,7′-bis(2-ethylhexyl)benzo[1′,2′-*c*:4′,5′-*c*']dithiophene-4,8–dione)]:3,9-bis(2-methylene-((3-(1,1-dicyanomethylene)−6/7-methyl)-indanone))−5,5,11,11-tetrakis(4-hexylphenyl)-dithieno[2,3-*d*:2′,3′-*d*']-*s*-indaceno[1,2-*b*:5,6-*b*']dithiophene (PBDB-T:IT-M) system with an inverted device structure have been fabricated to investigate the influence of 2PACz SAM on the device performance and stability (the chemical structures of PBDB-T and IT-M are detailed in Fig. S1 in Supporting information). We find that devices modified by 2PACz SAM have absolute advantages over the control devices in terms of photovoltaic parameters and stability. Compared with control devices with ZnO (or ZnO/PEIE) as the EEL, devices modified by 2PACz SAM (*i.e.*, ZnO/PEIE/2PACz) demonstrate a power conversion efficiency enhancement from 10.39% (or 10.72%) to 11.71%, and the efficiency remains at about 88% of its initial value after storage in the air for more than 500 h. All in all, we provide a new strategy of using self-assembled 2PACz monolayer as an interface layer to fabricate high-performance and stable non-fullerene OSCs.

The chemical structures and binding bonds of PEIE and 2PACz are shown in Fig. 1a. A solution of 2PACz in methanol (0.3 mg/mL) was spin-coated onto the surface of PEIE covered ZnO, then a self-assembled monolayer of 2PACz could be formed due to the strong hydrogen bonds between the phosphoryl group of 2PACz and the hydroxyl group of PEIE, together with covalent bonds connection between the hydroxyl group of PEIE and the phosphonic acid headgroup of 2PACz by dehydration condensation reaction [28,29]. PEIE is a kind of polymer with plenty of hydroxyl groups, which can both smooth the surface of ZnO and provide plenty of binding sites for 2PACz. As shown from the ultraviolet-visible (UV–vis) absorption spectra (Fig. 1b), after the modification of ZnO/PEIE with a 2PACz SAM, the characteristic absorption peak of carbazole group appears at 300 nm [30]. We utilize ultraviolet photoelectron spectroscopy (UPS) to characterize the change of electrode work function (WF) before and after 2PACz modification. The binding energies of ZnO, ZnO/PEIE and ZnO/PEIE/2PACz layers are shown in Fig. 1c, the WFs of ITO covered by ZnO, ZnO/PEIE and ZnO/PEIE/2PACz are calculated to be 4.06, 3.28 and 3.59 eV, respectively, by using the equation: $WF = h\nu - E_{cutoff}$, and the data are summarized in Table 1. After 2PACz modification (*i.e.*, ZnO/PEIE/2PACz), the WF reduces by 0.47 eV relative to ZnO but increases by 0.31 eV relative to ZnO/PEIE, indicating the existence of strong interfacial dipole effect. The WF of ZnO/ 2PACz layers are 4.19 eV (Fig. S2 in Supporting information). The lower WF of the cathode covered by ZnO/PEIE/2PACz relative to ZnO will be beneficial to improving the electron extraction. The elevation of WF for ZnO/PEIE/2PACz relative to ZnO/PEIE may be partially attributed to the reduction of dipole of the interlayer when the PEIE surface is covered by 2PACz.

The contact angle test also confirms that PEIE and 2PACz successfully cover the surface of ZnO layer. The consequences of water contact angle measurements are shown in Fig. 2, and those of the oil contact angles are shown in Fig. S3 (Supporting information). The water contact angles vary from 44.4° on ZnO to 48.8° on ZnO/PEIE and then largely change to 59.4° on ZnO/PEIE/2PACz due to the hydrophobic nature of the carbazole group in 2PACz.

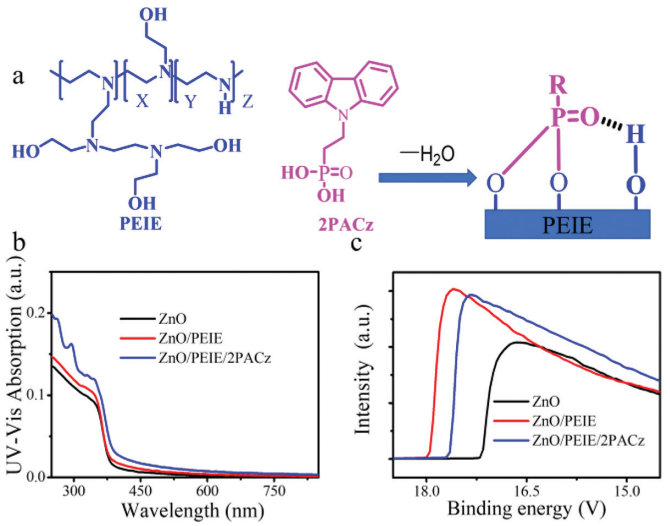

Fig. 1. (a) Chemical structures and bonds connections of PEIE and 2PACz. (b) UV–vis absorption spectra of ZnO, ZnO/PEIE, ZnO/PEIE/2PACz films on the quartz plate. (c) UPS profiles of ZnO, ZnO/PEIE, ZnO/PEIE/2PACz films on silicon wafer.

Table 1
Summary of WFs and surface energies of EELs.

EEL	WF (eV)	γ_s (mN/m)
ZnO	4.06	64.5
ZnO/PEIE	3.28	54.3
ZnO/PEIE/2PACz	3.59	44.2

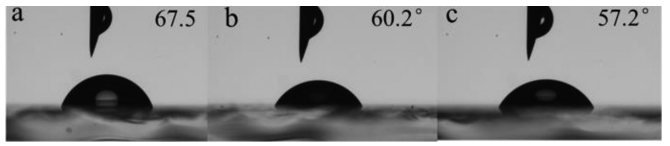

Fig. 2. The water contact angles on different surfaces: (a) ZnO, (b) ZnO/PEIE, (c) ZnO/PEIE/2PACz.

Table 2
Photovoltaic parameters of PBDB-T:IT-M based OSCs with different EELs under the irradiation of AM 1.5 G 100 mW/cm^2 light.

EEL	V_{oc} (V)	J_{sc} (mA/cm^2)	J_{cal} (mA/cm^2)[a]	FF (%)	PCE (%)	$PCE_{average}$ (%)	R_s (Ω cm^2)
ZnO	0.923	16.05	15.54	70.37	10.39	10.25±0.06	7.68
ZnO/PEIE	0.930	16.16	15.82	71.58	10.72	10.64±0.04	6.88
ZnO/PEIE/2PACz	0.923	17.55	16.58	72.55	11.71	11.58±0.11	5.84

[a] J_{cal} stands for the short-circuit current density calculated from the EQE measurement.

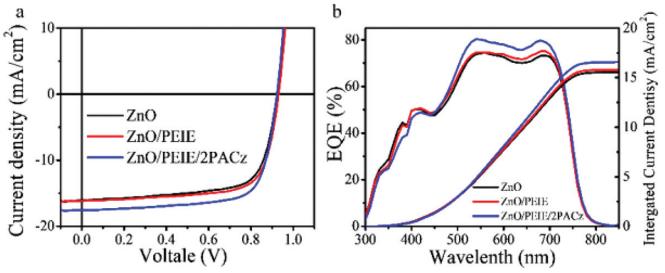

Fig. 3. (a) *J-V* curves and (b) EQE spectra of PBDB-T:IT-M based OSCs using ZnO, ZnO/PEIE and ZnO/PEIE/2PACz as the EEL.

The surface energy of ITO/EEL is also a factor that affects the morphology of photoactive layer in OSCs. So, we further calculate the surface free energy from the contact angle measurements. As shown in Table 1, the results demonstrate that the surface free energy (44.2 mN/m) of ZnO/PEIE/2PACz EEL is lower than those of ZnO/PEIE (54.3 mN/m) and ZnO (64.5 mN/m). It is reported that the degree of molecular ordering and extent of domain alignment increase with the decrease in the substrate surface energy [31], which will be beneficial to the charge carrier transport. In addition, the lower WF can be more favorable for electron extraction at the cathode side. Therefore, we expect the 2PACz modified EEL can be used in OSCs for photovoltaic performance improvement. Furthermore, the surface morphology and composition of the ZnO/PEIE/2PACz EEL are analysed by scanning electron microscopy (SEM) and energy dispersive X-ray (EDX) spectroscopy, respectively. As shown in Fig. S4 (Supporting information), the distribution of P element (Fig. S4e) on ZnO/PEIE/2PACz verifies that the coverage of 2PACz SAM is uniform. Combined with all the above evidences, we know that 2PACz successfully modifies the surface of ZnO/PEIE.

To test the photovoltaic performance, OSCs with an inverted device structure (ITO/EEL/PBDB-T:IT-M/MoO_3/Ag) were fabricated, where EEL stands for ZnO, ZnO/PEIE, or ZnO/PEIE/2PACz. The current density-voltage (*J-V*) curves are shown in Fig. 3a. Table 2 summarizes device performances with different cathode modification layers measured under the illumination of AM 1.5 G (100 mW/cm^2) light source. ZnO-only OSCs exhibit a PCE of 10.39% with an open-circuit voltage (V_{oc}) of 0.923 V, a short-circuit current density (J_{sc}) of 16.05 mA/cm^2 and a fill factor (FF) of 70.37%, which are close to the values described in the literature [31]. In contrast, the PCEs of OSCs modified by PEIE and PEIE/2PACz interlayer are increased to 10.72% and 11.71%, respectively. Compared with the ZnO-only devices, the V_{oc} values are almost unchanged; whereas the J_{sc} values of PEIE and PEIE/2PACz modified devices are increased from 16.05 mA/cm^2 to 16.16 mA/cm^2 and 17.55 mA/cm^2, respectively. The reason is inseparable from the reduction of work function after the modification of cathode with PEIE or PEIE/2PACz, which will facilitate the electron extraction by the electrode. At the same time, the decrease of surface free energy is beneficial to increasing the degree of molecular ordering and the extent of domain alignment of the active layer [32], thus boosting the FF. Interestingly, the series resistance (R_s) value is lower in PEIE/2PACz based devices (5.84 Ω cm^2) than that in devices with PEIE (6.88 Ω cm^2) or without interlayer (7.68 Ω cm^2).

Table 3
Hole and electron mobility and their ratio in PBDBT:IT-M devices based on different EELs.

EEL	μ_h (cm^2 V^{-1} s^{-1})	μ_e (cm^2 V^{-1} s^{-1})	μ_h/μ_e
ZnO	1.9×10^{-4}	0.85×10^{-4}	2.0
ZnO /PEIE	1.9×10^{-4}	1.38×10^{-4}	1.37
ZnO /PEIE/2PACz	1.9×10^{-4}	1.68×10^{-4}	1.13

The increase in J_{sc} after interlayer modification can also be reflected in EQE curves. As shown in Fig. 3b and Fig. S5 (Supporting information), devices with the PEIE and PEIE/2PACz interlayer exhibit a particularly stronger response in the wavelength range of 450–700 nm relative to those without the interlayer (ZnO-only devices), especially for the latter. This result coincides with the J_{sc} increase in PEIE based devices which is not as large as that in PEIE/2PACz based ones. In particular, the EQE of PEIE/2PACz based devices can reach a maximum value of 80% at 540 nm, and its response in the range of 510–710 nm is above 70% corresponding to the contribution of light absorption of both PBDB-T and IT-M.

The carrier mobility and recombination of these devices are discussed on account of the FF differences. As shown in Fig. 4a, the J_{sc} value as a function of the light intensity (P_{light}) is fitted by the power-law relationship $J_{sc} \propto P_{light}^{\alpha}$ (α is an index factor) to get the α value of 0.833, 0.855 and 0.865 for ZnO, ZnO/PEIE, and ZnO/PEIE/2PACz based devices, respectively. When α is close to 1, it indicates that the bimolecular recombination in the donor: acceptor blend film can be ignored [33]. OSCs with interlayers demonstrate a higher α value than ZnO-only devices, especially for PEIE/2PACz based devices, which have a much higher α value. The above results demonstrate that the bimolecular combination can be suppressed to some extent in devices modified with interlayers and explain the FF differences in devices with different interlayers.

The space-charge-limited-current (SCLC) method is used to determine the hole (μ_h) and electron (μ_e) mobilities. The device structures for measuring hole and electron mobilities are ITO/PEDOT:PSS/active layer/MoO_3/Ag and ITO/EEL/active layer/PDINO/Ag, respectively [34,35]. As presented in Table 3 and Fig. S6 (Supporting information), OSCs based on ZnO, ZnO/PEIE, and ZnO/PEIE/2PACz EEL display similar hole mobilities; while the electron mobilities are markedly increased after the modification. OSCs with PEIE/2PACz interlayer exhibit the highest electron mobility among these three different kinds of devices, resulting in the most balanced μ_h/μ_e ratio. The introduction of 2PACz SAM slightly inhibits the bimolecular recombination of carriers, greatly improves the electron mobilities, and thus improves the FF, J_{sc} and PCE of OSCs.

To understand the increase of J_{sc} and FF after 2PACz SAM modification, we explored the transient photocurrent (TPC), photovoltage (TPV) and the relationship between photocurrent density (J_{ph}) and effective voltage (V_{eff}) of OSCs [36–38]. The results are shown in Fig. 4b and Fig. S7 (Supporting information). The exciton dissociation efficiency can be characterized by normalized photocurrent density ($\eta_{diss} = J_{ph}/J_{sat}$, J_{sat} is the saturated photocurrent density), when the OSC is in the short circuit condition. As listed in Fig. 4b,

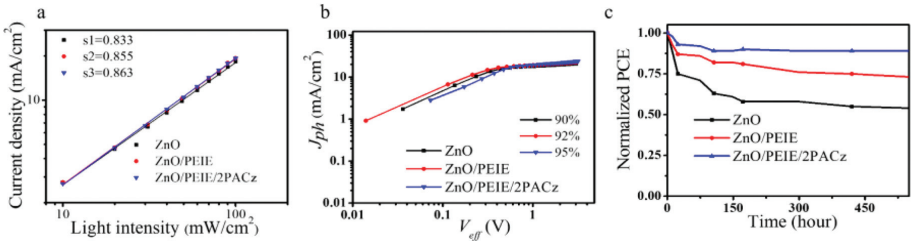

Fig. 4. (a) Photocurrent density-incident light intensity curves, (b) J_{ph} *versus* V_{eff} curves, and (c) the air stability of PBDB-T:IT-M based OSCs using ZnO, ZnO/PEIE and ZnO/PEIE/2PACz as the EEL.

the η_{diss} values of OSCs with ZnO, ZnO/PEIE and ZnO/PEIE/2PACz EEL are determined to be 90%, 92% and 95%, respectively, which proves that the exciton dissociation and charge separation ability are improved after the introduction of the interlayers. Therefore, the J_{SC} and FF of OSCs are increased.

We use TPV and TPC techniques to study the charge recombination kinetics of OSCs with different interface layers [39,40]. As shown in Fig. S7a, under the open-circuit condition, the TPV signals of the three kinds of devices are compared. The carrier lifetimes are calculated by fitting the TPV curve with a single-exponential decay to be 5.9, 32.8 and 58.2 μs for devices based on ZnO, ZnO/PEIE and ZnO/PEIE/2PACz interlayers, respectively. The ZnO/PEIE/2PACz based devices show the longest carrier lifetime and the weakest charge recombination, indicating that the interface traps can be passivated by 2PACz SAM. Similarly, we tested the TPC of OSCs under short-circuit condition and calculated the charge extraction time (τ_e). As shown in Fig. S7b, the ZnO/PEIE/2PACz based device exhibits the shortest τ_e value (320 ns), which is much smaller than 480 ns of ZnO and 370 ns of ZnO/PEIE based devices. The fast carrier extraction rate indicates that the charge carrier recombination is reduced and the charge extraction from the BHJ layer is improved in devices with 2PACz SAM modification, which is consistent with the J_{ph}-V_{eff} result. From the above results we can conclude that the interface defects after the 2PACz modification can be suppressed and 2PACz can form a strong interface dipole on PEIE to change the interface work function which promote the extraction of electrons relative to the ZnO-only devices.

The air stability of OSCs with different interfacial layers was investigated, as it is essential for future practical application. We continue to measure the PCE of OSCs after they were taken out of the glove box without encapsulation and stored in the ambient condition (air) for a certain time. The normalized PCE drawn as a function of retention time in air is shown in Fig. 4c. After 555 h of continuous storage in air, the ZnO/PEIE/2PACz-based OSC retains ~90% of its initial PCE; while PCEs of ZnO-only and ZnO/PEIE-based OSCs deteriorate to 60% and 70% of their initial values, respectively, after 150 h storage in air. These results indicate that the 2PACz SAM interlayer can help to prolong the storage lifetime of OSCs. The light stability of OSCs with different interfacial layers was investigated. We continue to measure the PCE of OSCs under the irradiation of 100 mW/cm^2 tungsten lamp light in the glove box. After 96 h, the ZnO/PEIE/2PACz-based OSC retains ~75% of its initial PCE; while PCEs of ZnO-only and ZnO/PEIE-based OSCs deteriorate to 55% and 65% of their initial values, respectively (Fig. S8 in Supporting information).

In summary, we modified the ZnO layer with a 2PACz SAM to improve the photovoltaic performance of inverted OSCs. The 2PACz SAM modification can greatly reduce the surface free energy and the surface defects of EEL. And 2PACz can form a strong interface dipole on EEL to change the interface work function and to promote the extraction of electrons. As a result, the PCE of PBDB-T:IT-M based OSCs is increased from 10.39% to 11.71% with its stability in the air greatly improved as compared with devices without 2PACz modification. After 2PACz modification, the photostability and air stability of the devices have been significantly improved. Even after storage in air for 555 h, the device efficiency can still remain 88% of its initial value. All in all, we demonstrate that 2PACz modification is an effective new strategy for constructing high-performance OSCs with markedly enhanced air stability.

Declaration of competing interest

There are no conflicts to declare.

Acknowledgment

Financial support from the National Natural Science Foundation of China (No. 51973020) is acknowledged.

Supplementary materials

Supplementary material associated with this article can be found, in the online version, at doi:10.1016/j.cclet.2022.05.009.

References

[1] R. Søndergaard, M. Hösel, D. Angmo, T.T. Larsen-Olsen, F.C. Krebs, Mater. Today 15 (2012) 36–49.
[2] A. Prasetio, M. Jahandar, S. Kim, et al., Adv. Sci. 8 (2021) 2100865.
[3] Y. Cui, H. Yao, J. Zhang, et al., Adv. Mater. 32 (2020) 1908205.
[4] H. Lu, J. Liu, Y. Liu, X. Xu, Z. Bo, ChemSusChem 14 (2021) 5442–5449.
[5] J. Yuan, Y. Zhang, L. Zhou, et al., Joule 3 (2019) 1140–1151.
[6] W. Liu, J. Wang, Y. Gong, et al., Angew. Chem. Int. Ed. 59 (2020) 20161–20166.
[7] M. Liu, P. Fan, Q. Hu, T.P. Russell, Y. Liu, Angew. Chem. Int. Ed. 59 (2020) 18131–18135.
[8] J. Wang, Z. Zheng, D. Zhang, et al., Adv. Mater. 31 (2019) 1806921.
[9] Z. Zheng, Q. Hu, S. Zhang, et al., Adv. Mater. 30 (2018) 1801801.
[10] K. Zhang, C. Zhong, S. Liu, et al., ACS Appl. Mater. Interfaces 6 (2014) 10429–10435.
[11] C. Li, J. Zhou, J. Song, et al., Nat. Energy 6 (2021) 605–613.
[12] S.W. Baek, J.H. Kim, J. Kang, et al., Adv. Energy Mater. 5 (2015) 1501393.
[13] Y. Han, H. Dong, W. Pan, et al., ACS Appl. Mater. Interfaces 13 (2021) 17869–17881.
[14] Q. Liao, Q. Kang, Y. Yang, et al., CCS Chem. (2021) 1059–1069.
[15] J. Xiao, X. Jia, C. Duan, et al., Adv. Mater. 33 (2021) 2008158.
[16] P. Fu, X. Guo, B. Zhang, et al., J. Mater. Chem. A 4 (2016) 16824–16829.
[17] S. Cho, K.D. Kim, J. Heo, et al., Sci. Rep. 4 (2014) 4306.
[18] L. Yan, Y. Song, Y. Zhou, B. Song, Y. Li, Org. Electron. 17 (2015) 94–101.
[19] S. Nam, J. Seo, S. Woo, et al., Nat. Commun. 6 (2015) 8939.
[20] Y. Tan, L. Chen, F. Wu, et al., Macromol 51 (2018) 8197–8204.
[21] G. Pace, A. Grimoldi, D. Natali, et al., Adv. Mater. 26 (2014) 6773–6777.
[22] L. Hu, Y. Liu, L. Mao, et al., J. Mater. Chem. A 6 (2018) 2273–2278.
[23] A. Al-Ashouri, E. Kohnen, B. Li, et al., Science 370 (2020) 1300–1309.
[24] M. Ross, L. Gil-Escrig, A. Al-Ashouri, et al., ACS Appl. Mater. Interfaces 12 (2020) 39261–39272.
[25] A. Al-Ashouri, A. Magomedov, M. Roß, et al., Energy Environ. Sci. 12 (2019) 3356–3369.
[26] Y. Lin, Y. Firdaus, F.H. Isikgor, et al., ACS Energy Lett. 5 (2020) 2935–2944.
[27] P.J. Hotchkiss, S.C. Jones, S.A. Paniagua, et al., Acc. Chem. Res. 45 (2012) 337–346.
[28] Y. Lin, Y. Firdaus, F.H. Isikgor, et al., ACS Energy Lett. 5 (2020) 2935–2944.
[29] S.P. Pujari, L. Scheres, A.T.M. Marcelis, H. Zuilhof, Angew. Chem. Int. Ed. 53 (2014) 6322–6356.
[30] M. Ross, L. Gil-Escrig, A. Al-Ashouri, et al., ACS Appl. Mater. Interfaces 12 (2020) 39261–39272.

[31] W. Jiang, R. Yu, Z. Liu, et al., Adv. Mater. 30 (2018) 1703005.
[32] F. Zhang, E. Mohammadi, X. Luo, et al., Langmuir 34 (2018) 1109–1122.
[33] Y. Zhou, M. Li, H. Lu, et al., Adv. Funct. Mater. 31 (2021) 2101742.
[34] Y. Zhang, C.e. Zhang, H. Huang, et al., Dyes Pigm. 184 (2021) 4–24.
[35] X. Wang, H. Lu, J. Zhou, et al., ACS Appl. Mater. Interfaces 13 (2021) 39652–39659.
[36] Y.N. Chen, R. Zheng, J. Wang, et al., J. Mater. Chem. C 9 (2021) 6937–6943.
[37] X. Du, Y. Yuan, L. Zhou, et al., Adv. Funct. Mater. 30 (2020) 1909837.
[38] V.D. Mihailetchi, H.X. Xie, B. de Boer, L.J.A. Koster, P.W.M. Blom, Adv. Funct. Mater. 16 (2006) 699–708.
[39] C. Sun, S. Qin, R. Wang, et al., J. Am. Chem. Soc. 142 (2020) 1465–1474.
[40] H. Xu, H. Zou, D. Zhou, et al., ACS Appl. Mater. Interfaces 12 (2020) 52028–52037.